Simultaneous Gradient-Echo/Spin-Echo EPI of Graded Ischemia in Human Skeletal Muscle

Kathleen M. Donahue, PhD • Joel Van Kylen, BS • Safak Guven, MD • Ahmed El-Bershawi, MD
Wen-Ming Luh, MS • Peter A. Bandettini, PhD • Robert W. Cox, PhD • James S. Hyde, PhD
Ahmed H. Kissebah, MD, PhD

The goal of this study was to evaluate the usefulness of blood oxygenation level–dependent (BOLD) methodologies to provide temporal and spatial information about skeletal muscle perfusion. A simultaneous gradient echo (GE) and spin-echo (SE) imaging sequence (GE/SE) with alternating TE was used to acquire images of leg skeletal muscle throughout a stepped reactive hyperemia paradigm. The change in both the GE and SE relaxation rates ($\Delta R2^*$, $\Delta R2$) measured during ischemia and reactive hyperemia scaled with the duration of cuff inflation (the ischemic period) plateaued for cuff inflations lasting longer than 120 seconds and were greater in soleus muscle than in gastrocnemius. The ratio $\Delta R2^*/\Delta R2$ was found to be less during the reactive hyperemia period relative to ischemia. Considering that a greater proportion of capillary vessels are perfused during reactive hyperemia than during ischemia, this finding suggests that magnetic susceptibility methodologies, with their dependence on compartment size, may provide a measure of the relative distribution of small and large vessels in skeletal muscle.

Index terms: Skeletal muscle perfusion • Insulin • BOLD • FMRI

JMRI 1998; 8:1106–1113

Abbreviations: ANOVA = analysis of variance, BOLD = blood oxygenation level–dependent, EPI = echo planar imaging, FOV = field of view, GE = gradient echo, RF = radiofrequency, ROI = region of interest, SE = spin echo

From the Biophysics Research Institute (K.M.D., J.V.K., W.-M.L., P.A.B., R.W.C., J.S.H.) and the Department of Medicine, Endocrine Division (K.M.D., S.G., A.E.-B., A.H.K.), Medical College of Wisconsin, 8701 Watertown Plank Road, Milwaukee, WI 53226. E-mail: kathleen@mcw.edu. Received October 6, 1997; revision requested February 9, 1998; revision received March 11, 1998; accepted March 25, 1998. This work was supported in part by grants from the National Institutes of Health (HL34989-07) and the Medical College of Wisconsin Research Affairs Committee. Presented in part at the 5th scientific meeting and exhibition of the International Society for Magnetic Resonance in Medicine, Vancouver, April 12–18, 1997. **Address reprint requests to** K.M.D.

© ISMRM, 1998

THE EVALUATION of the spatial and temporal aspects of skeletal muscle perfusion is relevant to our understanding of several common disease states, obesity, type 2 diabetes mellitus, and hypertension. Each of these disease states exhibits resistance to insulin's action to stimulate glucose uptake in skeletal muscle, the primary site of glucose disposal. However, the fundamental mechanisms underlying insulin actions and resistance are not well understood. In particular, whether the major determinant of insulin action results from hemodynamic or cellular effects remains controversial (1–8). At the center of this controversy is our lack of understanding of the link between the hemodynamic and metabolic changes, in particular the spatial and temporal aspects of perfusion, with the possibility of a spatially heterogeneous response to insulin (9). Although currently available methods such as strain-gauge plethysmography (10,11), radioactive tracer (12), and thermodilution techniques (13) provide information related to bulk blood flow, they do not provide temporal and spatial perfusion information. And although electromagnetic flow recordings (14), pulsed ultrasound-Doppler, and laser-Doppler flowmetry (15) methods provide temporal perfusion information, only localized areas can be measured at any given time.

Alternatively, MR functional imaging techniques not only provide detailed spatial information but more recently, with the advent of fast imaging techniques such as fast gradient echo (GE) and echo planar imaging (EPI), have the time resolution necessary to evaluate fast physiologic processes such as perfusion. A particularly successful functional MRI technique relies on the blood oxygenation level–dependent (BOLD) effect (16), which is sensitive to alterations in local deoxyhemoglobin content. This technique has become a mainstay of human brain activation studies (see refs. 17 and 18). In these studies, it is thought that neuronal activation within the cerebral cortex results in increases in local cerebral blood flow without a commensurate increase in the oxygen consumption rate, thereby causing a decrease in capillary and venous deoxyhemoglobin concentrations and hence increases in T2*/T2-weighted MR signal and BOLD contrast. Subsequently, BOLD signal changes have also been shown to correlate with perfusion changes in other organs such as kidney (19), cardiac tissue (20,21), and more recently skeletal muscle (22–24).

An added advantage of using BOLD techniques is the variable sensitivity of BOLD imaging sequences to compartment size. In particular, recent results from both numerical simulations (25,26) and measurements (27,28) indicate that spin-echo (SE) and GE images have greatly differing sensitivities to the size scale of the field inhomogeneities. A consequence of this difference is that the SE signal change (characterized by the change in the T2 rate, $\Delta R2$) is maximally sensitive to compartments with dimensions approximately equal to the dimensions of capillaries, whereas the GE signal ($\Delta R2^*$) is roughly equally sensitive to all vessel sizes. Also, there is both theoretical and experimental evidence to indicate that the ratio of GE to SE relaxation rate changes ($\Delta R2^*/\Delta R2$) is, to first order, proportional to the tissues' average vessel size (26,29–31). Therefore, measurement of this ratio may provide information related to the relative distribution of small and large vessels and therefore vascular redistribution.

The goal of this study was to evaluate the usefulness of BOLD methodologies to provide temporal and spatial information about skeletal muscle total perfusion, microperfusion, and vascular redistribution. To accomplish this goal, a simultaneous GE and SE imaging sequence (GE/SE) (32,33) with alternating TE (34) was used to acquire images of leg skeletal muscle throughout a stepped reactive hyperemia paradigm, where the duration of ischemia is systematically increased or decreased. The GE/SE sequence enables the simultaneous acquisition of both total and microvascular perfusion information and provides the measurements necessary for calculating the ratio of GE to SE relaxation rate changes ($\Delta R2^*/\Delta R2$). Simultaneous acquisition is necessary to avoid systematic errors, resulting from system status or physiologic changes, that might occur between experiments, a case in point being the stepped reactive hyperemia paradigm used in this study. Reactive hyperemia was chosen as our test paradigm since it is a well-studied condition of skeletal muscle in which the perfusion response has been shown to scale with ischemia duration and an internal redistribution of the blood occurs during reactive hyperemia, so that capillary-sized vessels comprise a larger proportion of the perfused vessels.

• MATERIALS AND METHODS

Four healthy volunteers, two men and two women between the ages of 25 and 27, were studied in the supine position under resting conditions, during ischemia and reactive hyperemia produced in the lower leg. Ischemia was achieved with a sphygmomanometer cuff placed just proximal to the knee, connected to a rapid cuff inflator (D.E. Hokanson, Bellevue, WA) and inflated to 300 mm Hg in less than 1 second. The rapid inflation avoids any volume change in the venous compartment (22). For each volunteer, images were acquired throughout 1 minute of baseline, during ischemia, and for 3 minutes after ischemia, during which the reactive hyperemic response takes place. This experiment was repeated five times per subject, with the duration of ischemia lasting either 30, 60, 120, 180, or 300 seconds, with approximately 5 to 6 minutes between experiments. The order of the experiments was either reverse (subjects 1 and 2: 300 seconds down to 30 seconds) or increasing (subjects 3 and 4: 30 seconds up to 300 seconds).

Imaging

MRI was performed on a 3.0-T Bruker Biospec System (Karlsruhe, Germany) fitted with a home-built 8.5-in local three-axis gradient coil and a quadrature transmit-receive birdcage radiofrequency (RF) coil. GE sagittal scout images were obtained and an axial slice was chosen at midcalf so that the gastrocnemius and soleus muscles were both present within a single 10-mm imaging slice. Subsequently, a high-resolution (256 × 256) SE image (field of view [FOV] = 16 cm, TR = 1,000 msec, TE = 30 msec) was obtained at the chosen axial position.

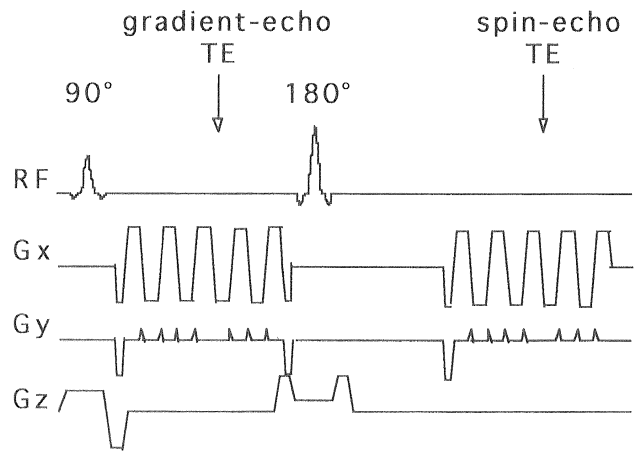

Figure 1. Simultaneous GE/SE-EPI sequence. The GE and SE images were acquired nearly simultaneously with TE = 27.2 and 109.1 msec, respectively. The sequence was then repeated with incremented TEs of 37.2 and 129.1 msec. Note that not all phase-encoding blips are shown. Also, at TE the ky = 0 line is acquired twice to enable phase correction.

During the reactive hyperemia paradigm, images were obtained using a simultaneous GE/SE-EPI sequence, with alternating TE. As illustrated in Figure 1, the GE and SE images were acquired nearly simultaneously with TE = 27.2 and 109.1 msec. Every other GE and SE image set was acquired with incremented TEs of 37.2 and 129.1 msec, respectively. The TR was 2 seconds, with an FOV of 16 cm and a matrix of 64 × 64, giving an in-plane resolution of 2.5 × 2.5 mm.

Analysis

As depicted in Figure 2, GE and SE signal time-course data were extracted from 10.0–12.5-mm² regions of interest (ROIs) within the lateral or medial gastrocnemius and soleus muscle groups. Assuming monoexponential T2* and T2 decay, the transverse relaxation rate changes [$\Delta R2^* = \Delta(1/T2^*)$ and $\Delta R2 = \Delta(1/T2)$] were calculated as a function of time as follows:

$$\Delta R2^* \text{ or } \Delta R2 = \frac{-1}{(TE)} \ln\left(\frac{S_a(t)}{S_r}\right) \qquad [1]$$

where S_r is the mean resting baseline GE or SE signal, and $S_a(t)$ represents either the GE or SE signal acquired at TEs of 27.2 and 109.1 msec during and after ischemia.

To evaluate whether $\Delta R2^*$ and $\Delta R2$ changes correlate with the perfusion changes known to occur during ischemia and reactive hyperemia, the areas under the $\Delta R2^*$ and $\Delta R2$ curves were determined for the last 30 seconds of cuff inflation (end-ischemia) and for 60 seconds beginning 6 seconds after cuff release (ie, during reactive hyperemia). This form of analysis was chosen since, as demonstrated with plethysmographic measures of blood flow (35), the amount of excess blood flowing during the hyperemic period is represented by the area between the

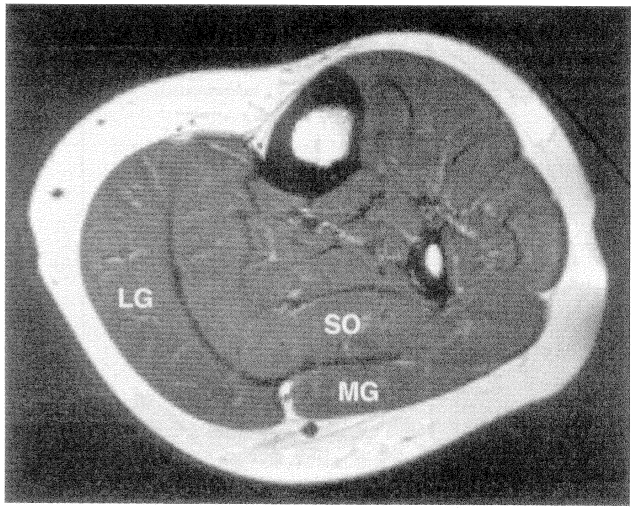

Figure 2. Conventional SE, high-resolution image of the leg cross section. GE and SE signal time-course data were extracted from 10.0–12.5-mm² ROIs within either the lateral or medial gastrocnemius (LG or MG) and soleus (SO) muscle groups.

curve of blood flow and resting level and was found to be linearly related to the duration of the ischemic period. Consequently, the means and standard errors of ΔR2* and ΔR2 areas, from all subjects, were determined and plotted as a function of ischemia duration for each muscle group.

Using the same ΔR2* and ΔR2 area data, end-ischemia and reactive hyperemia ΔR2*/ΔR2 ratios were determined for each muscle group as a function of ischemia duration. Single-factor analysis of variance (ANOVA) was used to determine whether the ratios differed significantly as a function of ischemia duration, at the .05 significance level. Last, a two-tailed *t* test was used to compare the ischemia and reactive hyperemia ratios.

Inherent to the determination of ΔR2* and ΔR2 as described by Equation [1] is the assumption that the equilibrium magnetization, M_o, remains unchanged. However, in practice, Mo can be influenced by T1 and therefore flow effects. Thus, to address the issue of whether flow changes affect the apparent M_o and therefore the observed relaxation rate changes, the apparent $M_o(t)$ was calculated from the same ROIs from which the ΔR2* and ΔR2 data were extracted. Specifically, using the alternating TE, GE data, the GE signals $S_1(t)$ and $S_2(t)$, acquired at TE_1 = 27.2 msec and TE_2 = 37.2 msec, respectively, are:

$$S_1(t) = M_o(t)\ \exp^{(-TE_1/T2(t))} \quad [2]$$

$$S_2(t) = M_o(t)\ \exp^{(-TE_2/T2(t))} \quad [3]$$

It is assumed that at any given time t, $M_o(t)$ and T2(t) are the same for $S_1(t)$ and $S_2(t)$, since these signals are acquired within 10 msec of each other. Consequently, Equations [2] and [3] can be used to solve for $M_o(t)$:

$$M_o(t) = S_2(t)\ \exp^{((1/\Delta TE)\ \ln(S_1(t)/S_2(t))} \quad [4]$$

where ΔTE = 10 msec. The mean $M_o(t)/M_{ob}(t)$ (from all subjects), where $M_{ob}(t)$ is the baseline $M_o(t)$ determined according to Equation [4] from $S_1(t)$ and $S_2(t)$ acquired under resting conditions, was determined for both end-ischemia and reactive-hyperemic conditions as a function of ischemia duration. Single-factor ANOVA, at a .05 significance level, was used to determine whether the results varied significantly as a function of ischemia duration.

• RESULTS

Representative ΔR2* and ΔR2 time-course data are shown in Figure 3 for the gastrocnemius and soleus muscles. Both ΔR2* and ΔR2 increased during ischemia and decreased during reactive hyperemia. Note the leveling of the response during cuff inflation as the duration of the inflation increases.

The mean ΔR2* (Fig. 4a) and ΔR2 (Fig. 4b) areas, determined during the last 30 seconds of ischemia and the first 60 seconds of reactive hyperemia, are shown as a function of ischemia duration for the soleus and gastrocnemius muscle groups. During ischemia, both ΔR2* and ΔR2 increase with ischemia duration and begin to level off for cuff inflations greater than 120 seconds. During the reactive hyperemia phase, both ΔR2* and ΔR2 decrease with ischemia duration, but to a level significantly less than noted during ischemia. For each condition and muscle group, the GE (ΔR2*) response is greater than the SE (ΔR2) response. Finally, a general observation in all subjects studied was the greater response in the soleus relative to the gastrocnemius muscle group.

The ΔR2*/ΔR2 determined from the total ΔR2* and ΔR2 areas computed during the last 30 seconds of ischemia are plotted as a function of ischemia duration in Figure 5. Single-factor ANOVA revealed that these ratios are significantly dependent on ischemia duration. Conversely, the ratios, calculated from the reactive hyperemia rates, did not vary significantly with ischemia duration (data not shown). An inability to detect a dependence may be due in part to the much lower sensitivity of the ΔR2* and ΔR2 response during reactive hyperemia. Consequently, to address the question of whether this ratio is different during ischemia and reactive hyperemia, a comparison was made for the 180- and 300-second experiments only (Fig. 6). The calculated means and standard errors for the gastrocnemius ratios during ischemia and reactive hyperemia are 3.24 ± 0.42 (n = 7) and 1.52 ± 0.82 (n = 5), respectively, which are not significantly different at the .05 significance level (P = .069) as determined by an unpaired, two-tailed *t* test. The values for soleus are 3.01 ± .24 (n = 7) and 1.84 ± .44 (n = 6), which are marginally significantly different (P = .03). (Note that the ratio was not calculated for the cases where ΔR2 was not significantly different from baseline, since dividing ΔR2* by approximately 0 would result in an indeterminate value for the ratio. This explains why the number of samples (n) included in the statistical comparisons is less than 7 in the reactive hyperemia results.)

Figure 7 depicts the M_o/M_{ob} results as a function of ischemia duration for end-ischemia (Fig. 7a) and during reactive hyperemia (Fig. 7b). Single-factor ANOVA revealed no significant dependence of the apparent magnetization on ischemia duration. In addition, the mean of all ischemic and reactive hyperemia M_o/M_b ratios was not significantly different as determined by a paired, two-tailed *t* test at the .05 significance level.

• DISCUSSION

These studies demonstrate that simultaneously acquired GE and SE images provide temporal and spatial information about skeletal muscle perfusion and potentially vascular redistribution. Specifically, the changes in the BOLD GE and SE signals were found to be consistent with perfusion changes that are known to occur during ischemia and reactive hyperemia. The relaxation rates

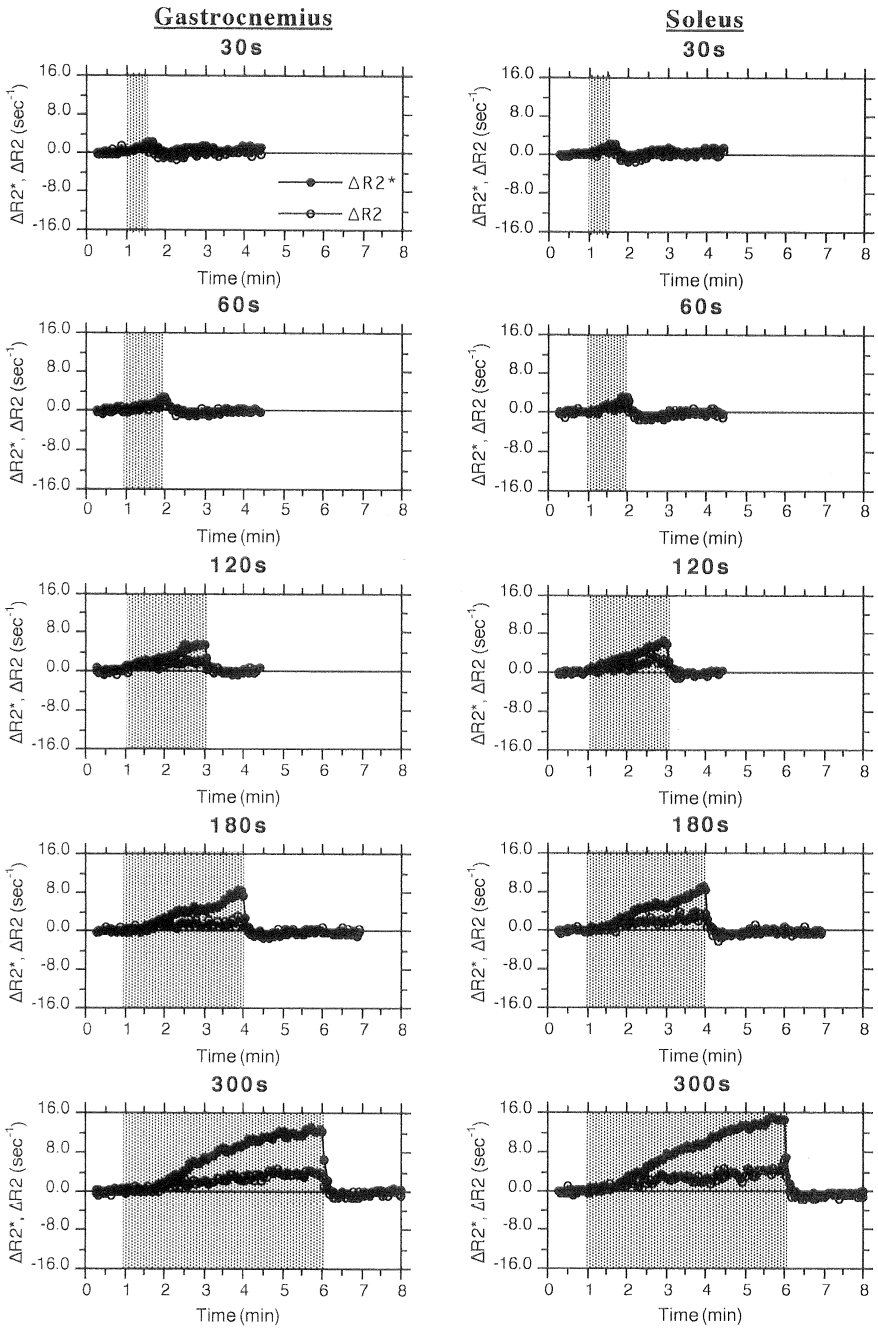

Figure 3. Representative ΔR2* (●) and ΔR2 (○) time-course data for gastrocnemius and soleus muscles. Consistent with our understanding of BOLD contrast, both ΔR2* and ΔR2 increase during ischemia, when an increase in deoxygenated blood is expected, and decrease during reactive hyperemia, when a decrease in deoxygenated blood is expected.

scale in direct proportion to the duration of cuff inflation, a finding consistent with the literature demonstrating increases in excess flow as the occlusion duration increases (36). Also, the responses varied significantly among the muscle groups, with the soleus muscle group having a greater response than the gastrocnemius. Differences in response are consistent with soleus being comprised of more red (oxidative) muscle fibers than the gastrocnemius, which has relatively more white (nonoxidative) muscle fibers. Red muscle fibers have greater capillary density, oxygen consumption, and blood flow rates than white fibers (37).

Additional information derived from using the GE/SE methodology includes a ΔR2*/ΔR2 ratio that increases with ischemia duration during cuff inflation and decreases during reactive hyperemia relative to ischemia. Given the theoretical and experimental evidence (25–28,38), which suggests that ΔR2* is approximately equally sensitive to vessels of all sizes, whereas ΔR2 is primarily sensitive to capillary-sized compartments, this result suggests an increase in the proportion of capillary-sized vessels during reactive hyperemia compared with ischemia. Assuming that this ratio is unaffected by changes in blood oxygenation, as has been demonstrated (39), these MRI findings are consistent with previous studies demonstrating an internal redistribution of blood between these two states. In particular, upon release of the cuff, a larger proportion of the vessels perfused are those concerned with tissue exchange, ie, capillary-sized vessels (40,41). Consequently, these findings demonstrate that magnetic susceptibility methodologies, with their dependence on compartment size, may facilitate dif-

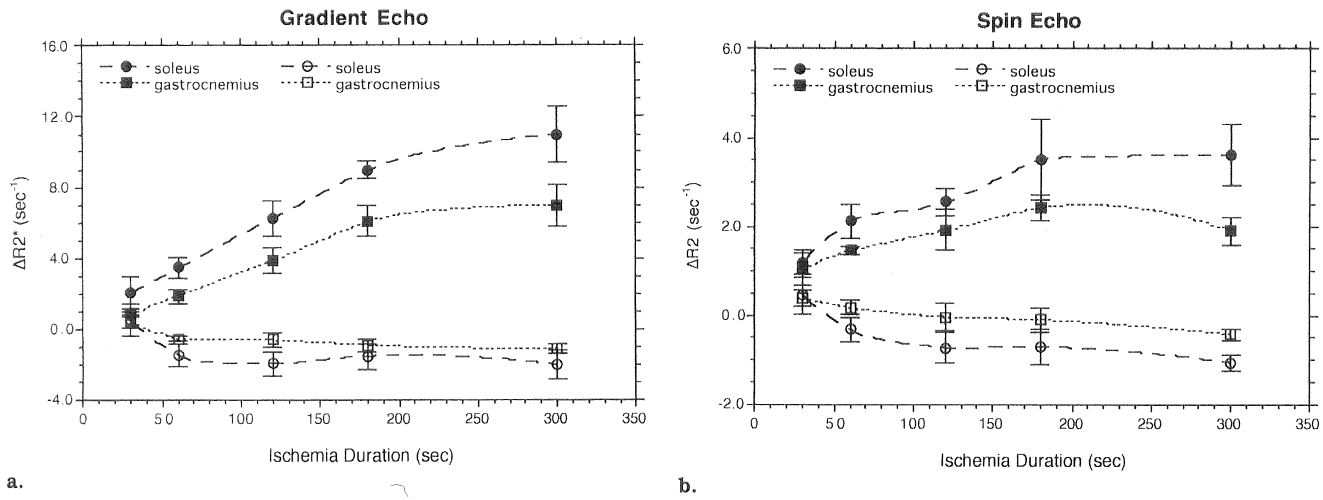

Figure 4. The ΔR2* **(a)** and ΔR2 **(b)** areas, determined during the last 30 seconds of ischemia (filled symbols) and the first minute of reactive hyperemia (open symbols) as a function of ischemia duration, for the soleus (●,○) and gastrocnemius (■,□) muscles. The data are given as the mean (from all four subjects) ± standard error of the mean. A general observation was the greater response in the soleus muscle relative to the gastrocnemius muscle during both end-ischemia and reactive hyperemia.

ferentiation of effects of the microvasculature from the macrovasculature.

Despite these intriguing results, it must be cautioned that the relationship between ΔR2*/ΔR2 and vessel size distribution is not yet fully understood. Specifically, most of the theoretical susceptibility models demonstrating the size dependence of GE and SE methodologies assumed extravascular susceptibility effects only. This assumption holds for studies using intravascular contrast agents, where the intravascular susceptibility effects are made negligible so that extravascular susceptibility effects dominate. Under such conditions, Dennie et al (29) demonstrated a significant correlation between ΔR2*/ΔR2 and averaged vessel size in brain relative to tumor. However, it has been recently demonstrated that intravascular susceptibility effects may be the dominant effect in BOLD studies, thus adding a more confusing size dependence to the GE/SE studies (42). Finally, it is not known whether the sensitivity of the SE sequence to red blood cells (which are also capillary-sized compartments) will result in a significant SE sensitivity to large vessels, which contain many small compartments (ie, red blood cells) (28). Studies addressing these issues are under way.

Although this report has demonstrated that BOLD techniques may be used as sensitive indicators of skeletal muscle perfusion changes, the fact that BOLD techniques are indirect indicators of perfusion must also be considered. Specifically, the success of using BOLD methodologies to evaluate perfusion changes is dependent on the maintenance of a blood-tissue oxygen gradient that is dominated by the blood oxygenation state. In addition to the oxygenation state of the blood, other factors, such as tissue O_2 consumption and myoglobin oxygen saturation, may contribute to or diminish BOLD contrast. For example, if increases in flow and therefore oxygenated blood are accompanied by commensurate increases in oxygen extraction, the susceptibility gradient will not be maintained, thereby making BOLD signal less perfusion dependent. This effect was observed in cardiac studies in which BOLD changes with dipyridamole, where myocardial oxygen supply (flow) exceeds demand, were much greater than those resulting from dobutamine stress, where the myocardial oxygen supply and demand

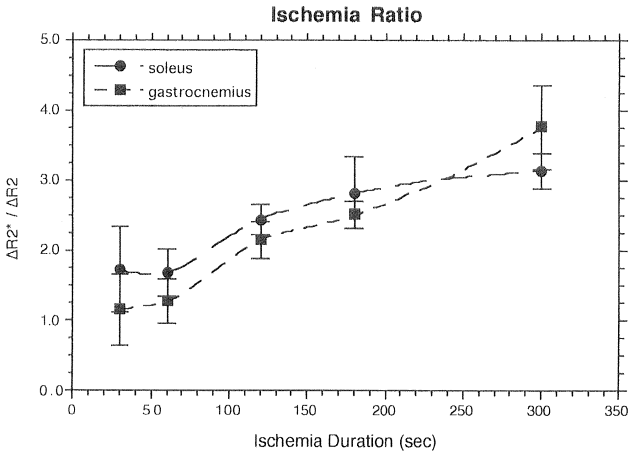

Figure 5. The mean ratio, ΔR2*/ΔR2, determined from the total ΔR2* and ΔR2 areas computed during the last 30 seconds of ischemia as a function of ischemia duration (time of cuff inflation). The ratios determined for both the soleus (●) and gastrocnemius (■) muscle groups demonstrate a statistically significant dependence on ischemia duration, as determined by single-factor ANOVA at the .05 significance level.

are balanced (43). Such may also be the case with exercise stress in skeletal muscle but apparently is not a dominant factor in this study, where signal decreased during ischemia and increased during reactive hyperemia. Additional evidence consistent with oxygen consumption's not being a dominant factor under reactive hyperemic conditions was presented by Fewings et al (44). An immediate transient fall in venous oxygen saturation was followed by a sustained rise in the oxygen saturation of venous blood draining from muscle after 1- to 10-minute periods of ischemia.

Another factor to consider when using BOLD contrast techniques to evaluate muscle perfusion is the oxygen saturation state of myoglobin. Since myoglobin resides in the muscle extravascular space, its saturation state can affect the blood-tissue oxygenation gradient and therefore the magnitude of the BOLD signal. For example, it has been shown that after approximately 1 minute of

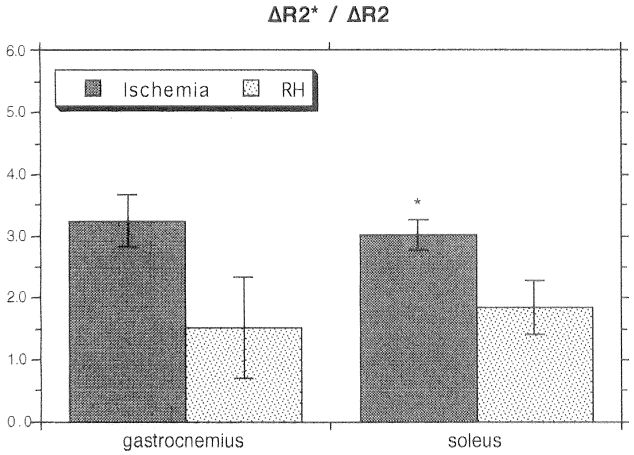

Figure 6. The mean ratio, ΔR2*/ΔR2, determined from the total ΔR2* and ΔR2 areas computed after cuff inflations of 180 and 300 seconds. The calculated means and standard errors for the gastrocnemius during ischemia and reactive hyperemia (RH) are 3.24 ± .42 (n = 7) and 1.52 ± .82 (n = 5), respectively, which are not significantly different at the .05 significance level (P = .069), as determined by an unpaired, two-tailed t test. The values for soleus are 3.01 ± .24 (n = 7) and 1.84 ± .44 (n = 6), which are significantly different (P = .03).

ischemia, myoglobin begins to desaturate, becoming fully desaturated after about 2–3 minutes of ischemia (23,45). Interestingly, the timing of desaturation seems to correlate with a leveling of the BOLD signal decrease during ischemia. This effect was also observed in this study after approximately 2 minutes of ischemia. One hypothesis explaining this finding is a simultaneous decrease in both hemoglobin and myoglobin oxygenation, thus leading to a leveling of the blood-tissue oxygenation gradient and a signal plateau. First-order approximations of blood-tissue susceptibility differences ($\Delta\chi$), with and without consideration of myoglobin desaturation, demonstrate that the myoglobin oxygenation state may decrease the BOLD response by as much as 50%, thus largely explaining the observed signal plateau (see Appendix).

An alternative or additional factor that may contribute to the ischemic signal plateau effect may be the attainment of a maximally vasodilated state, thus reaching a steady level of deoxyhemoglobin. However, measurements of tissue blood volume using near infrared spectroscopy demonstrate a blood volume that is relatively constant during the ischemic period but increased above baseline within 30 seconds after release of the occlusion (45). Still, it is interesting that, at least in the soleus muscle, the ΔR2*/ΔR2 ratio begins to plateau for higher durations of ischemia (Fig. 6). If this ratio is in fact an indicator of

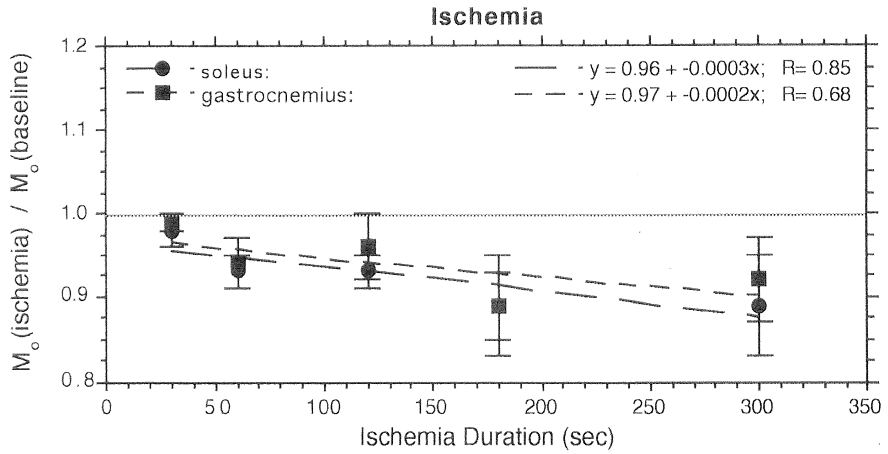

a.

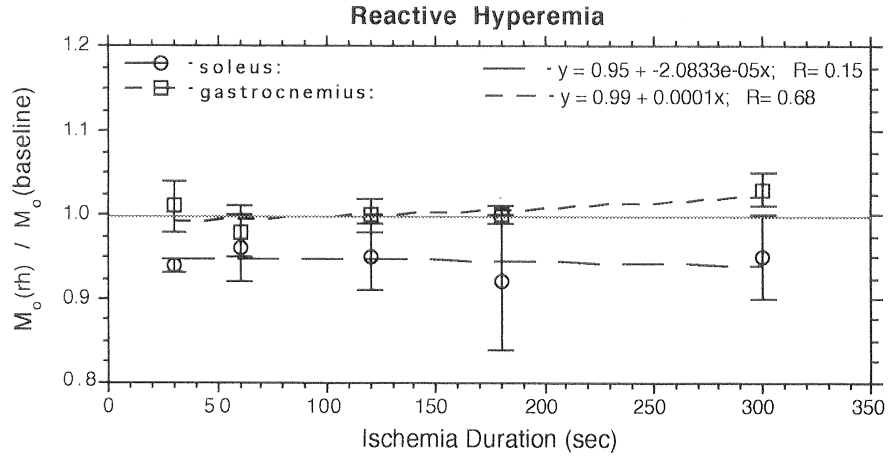

b.

Figure 7. M_o/M_{ob} results as a function of ischemia duration for end-ischemia **(a)** and during reactive hyperemia **(b)**. Single-factor ANOVA revealed no significant dependence of the apparent magnetization on ischemia duration. In addition, the means of all ischemic and reactive hyperemia M_o/M_b were not significantly different, as determined by a paired, two-tailed t test at the .05 significance level.

vessel size distribution, it may also be indicative of a maximally vasodilated state.

Although desaturation of myoglobin acts to decrease the observed ischemic BOLD contrast, a continued desaturation of myoglobin during reactive hyperemia would serve to increase the blood-tissue $\Delta\chi$ on release of the occlusion when an excess inflow of oxygenated blood occurs. However, it is well known that myoglobin becomes oxygenated almost immediately (46) and therefore probably does not contribute to the BOLD contrast observed during reactive hyperemia.

Finally, based on the finding that the apparent M_o does not change significantly either with ischemia duration or between ischemia and reactive hyperemia, the relaxation rate changes measured here are not influenced by flow changes that may affect T1 and therefore the apparent M_o. Ideally, to avoid any possibility of M_o influences, R2* and R2 rather than the relaxation rate changes (ΔR2* and ΔR2) should be calculated. Although the alternating TE sequence used here does provide the necessary information for this calculation, the sensitivity of the SE signal acquired at TE = 129.1 msec was not sufficient for the determination of R2, ie, differences in signal acquired at 109.1 and 129.1 msec were not detectable. To maximize SE sensitivity, the SE signal should be acquired at TE $\approx$T2. At 3 T the muscle T2 is approximately 60 msec. However, to enable the simultaneous acquisition of GE and SE sequence, 109.1 msec was the minimal SE TE. As a solution, a partial-NEX version of this sequence enabling SE acquisition at much shorter TE values will be used for future studies.

To summarize, the results of this study suggest that BOLD contrast imaging is useful in examining spatial and temporal perfusion changes in human skeletal muscle. The specific GE/SE methodology used here provides several advantages. First, both total and microvascular perfusion can be evaluated simultaneously. Second, the rapid and repetitive acquisition of images allows dynamic assessment of these changes. No other perfusion imaging modality is capable of determining time-dependent alterations with the temporal resolution of seconds or minutes. In addition, the combined GE and SE information has the potential to provide additional information related to vessel size distribution. This information is of extreme importance for the evaluation of insulin-resistant states associated with obesity and hypertension, where a rate-limiting step may be insulin's ability to redistribute microvascular perfusion.

• APPENDIX

With resting venous blood oxygenation levels of approximately 60% (44), the corresponding blood volume susceptibility relative to water is represented by $\Delta\chi$ and is 1.9×10^{-8} (47). This assumes a hematocrit of 40%, a $\Delta\chi$ for fully deoxygenated red blood cells of 1.57×10^{-7}, and a $\Delta\chi$ for fully oxygenated red blood cells of -0.26×10^{-7} (47). With profound ischemia, venous oxygenation levels drop almost completely, giving a blood $\Delta\chi$ of 6.3×10^{-8}. Assuming full oxygen saturation of tissue myoglobin in both the resting and ischemic states, the blood-tissue susceptibility difference would increase from 1.9×10^{-8} during rest to 6.3×10^{-8} during ischemia, an approximate threefold increase. Conversely, if myoglobin completely desaturates during ischemia, muscle $\Delta\chi$ would be approximately 2.1×10^{-8}, decreasing the ischemic blood-tissue susceptibility difference to 4.2×10^{-8}. [This assumes an upper-limit muscle myoglobin concentration of 3 times less than blood hemoglobin concentration. Muscle myoglobin concentrations are typically 3 to 10 times less than blood hemoglobin concentrations (46).] Consequently, the desaturation of myoglobin during ischemia may diminish the blood-tissue susceptibility changes by as much as 50%, thereby at least partially explaining the leveling of the BOLD signal during profound ischemia.

References

1. Baron AD. Hemodynamic actions of insulin. Am J Physiol 1994; 267:E187–E202.
2. Laakso M, Edelman SV, Brechtel G, Baron AD. Decreased effect of insulin to stimulate skeletal muscle blood flow in obese men. J Clin Invest 1990; 85:1844–1852.
3. Baron AD, Steinberg HO, Chaker H, Leaming R, Johnson A, Brechtel G. Insulin-mediated skeletal muscle vasodilation contributes to both insulin sensitivity and responsiveness in lean humans. Clin Invest 1995; 96:786–792.
4. Taddei S, Virdis A, Mattei P, Natali A, Ferrannini E, Salvetti A. Effect of insulin on acetylcholine-induced vasodilation in normotensive subjects and patients with essential hypertension. Circulation 1995; 92:2911–2918.
5. Natali A, Quinones G, Arzilli F, et al. Renovascular hypertension and insulin sensitivity. Eur J Clin Invest 1996; 26:556–563.
6. Bianchi S, Bigazzi R, Quinones G, et al. Insulin resistance in microalbuminuric hypertension: sites and mechanisms. Hypertension 1995; 26:789–795.
7. Paternostro G, Camici P, Lammerstma A, et al. Cardiac and skeletal muscle insulin resistance in patients with coronary heart disease: a study with positron emission tomography. J Clin Invest 1996; 98:2094–2099.
8. Natali A, Bonadonna R, Santoro D, et al. Insulin resistance and vasodilation in essential hypertension: studies with adenosine. J Clin Invest 1994; 94:1570–1576.
9. Clark MG, Colquhoun EQ, Rattigan S, et al. Vascular and endocrine control of muscle metabolism. Am J Physiol 1995; 268: E797–E812.
10. McKerslake D. The effect of the application of an arterial occlusion cuff to the wrist on the blood flow in the human forearm. J Physiol 1948; 108:451–457.
11. Sinoway LI, Hendrickson C, Davidson WR, Prophet S, Zelis R. Characteristics of flow-mediated brachial artery vasodilation in human subjects. Circ Res 1989; 64:32–42.
12. Lassen NA, Lindbjerg J, Munk O. Measurement of blood flow through skeletal muscle by intramuscular injection of Xenon-133. Lancet 1964; 28:686–689.
13. Andersen P, Saltin B. Maximal perfusion of skeletal muscle in man. J Physiol (Lond) 1985; 366:233–249.
14. Guldvog I, Kjaernes M, Thoresen M, Walloe L. Blood flow in arteries determined transcutaneously by an ultrasonic Doppler velocity meter as compared to electromagnetic measurements on the exposed vessels. Acta Physiol Scand 1980; 1090:211–216.
15. Larsson SE, Cai H, Zhang Q, Larsson R, Oberg PA. Measurement by laser-Doppler flowmetry of microcirculation in lower leg muscle at different blood fluxes in relation to electromyographically determined contraction and accumulated fatigue. Eur J Appl Physiol 1995; 70:288–293.
16. Ogawa S, Lee MT, Kay AR, Tank DW. Brain magnetic resonance imaging with contrast dependent on blood oxygenation. Proc Natl Acad Sci U S A 1990; 87:9868–9872.
17. Kwong KK, Belliveau JW, Chesler DA, et al. Dynamic magnetic resonance imaging of human brain activity during primary sensory stimulation. Proc Natl Acad Sci U S A 1992; 89:5675–5679.
18. Bandettini PA, Wong EC, Hinks RS, Tikofsky RS, Hyde JS. Time-course echo-planar imaging of human brain function during task activation. Magn Reson Med 1992; 25:390–397.
19. Prasad PV, Edelman RR, Epstein FH. Noninvasive evaluation of intrarenal oxygenation with BOLD MRI. Circulation 1996; 94: 3271–3275.
20. Wendland MF, Saeed M, Lauerma K, deCrespigny A, Moseley ME, Higgins CB. Endogenous susceptibility contrast in myocardium during apnea measured using gradient recalled echo planar imaging. Magn Reson Med 1993; 29:273–276.
21. Niemi P, Poncelet BP, Kwong KK, et al. Myocardial intensity changes associated with flow stimulation in blood oxygenation sensitive magnetic resonance imaging. Magn Reson Med 1996; 36:78–82.
22. Toussaint J-F, Kwong KK, M'Kparu F, Weisskoff RM, LaRaia PJ, Kantor HL. Perfusion changes in human skeletal muscle during reactive hyperemia measured by echo-planar imaging. Magn Reson Med 1996; 35:62–69.
23. Lebon V, Brillault-Salvat C, Bloch G, Leroy-Willig A, Carlier PG. The role of oxygen in functional imaging assessed by si-

multaneous interleaved gradient echo imaging and myoglobin spectroscopy during leg ischemia. In: Proceedings of the 4th annual meeting of the International Society for Magnetic Resonance in Medicine. New York: International Society for Magnetic Resonance in Medicine, 1996; 424.
24. Bandettini PA, Wong EC, Greene AS, Hinks RS, Hyde JS. Echo-planar and conventional imaging of signal attenuation in skeletal muscle during arterial compression. In: Proceedings of the 11th annual meeting of the Society of Magnetic Resonance in Medicine. Berlin: Society of Magnetic Resonance in Medicine, 1992; 321.
25. Fisel CR, Ackerman JL, Buxton RB, et al. MR contrast due to microscopically heterogeneous magnetic susceptibility: numerical simulations and applications to cerebral physiology. Magn Reson Med 1991; 17:336–347.
26. Boxerman JL, Hamberg LM, Rosen BR, Weisskoff RM. MR Contrast due to intravascular magnetic susceptibility perturbations. Magn Reson Med 1995; 34:555–566.
27. Majumdar S, Zoghbi S, Gore JC. The influence of pulse sequence on the relaxation effects of superparamagnetic iron oxide contrast agents. Magn Reson Med 1989; 10:289–301.
28. Bandettini PA, Wong EC, Jesmanowicz A, Hinks RS, Hyde JS. Spin-echo and gradient-echo EPI of human brain activation using BOLD contrast: a comparative study at 1.5T. NMR Biomed 1994; 7:12–20.
29. Dennie J, Mandeville JB, Weisskoff RM, Rosen BR. Quantitative imaging of tumor angiogenesis. In: Proceedings of the 5th annual meeting of the International Society for Magnetic Resonance in Medicine. Vancouver: International Society for Magnetic Resonance in Medicine, 1997; 489.
30. Bandettini PA, Wong EC. Effects of biophysical and physiologic parameters on brain activation-induced R2* and R2 changes: simulations using a deterministic diffusion model. Int J Imaging Sys Technol 1995; 6:133–152.
31. Ogawa S, Menon RS, Tank DW, et al. Functional brain mapping by oxygenation-dependent contrast magnetic resonance imaging: a comparison of signal characteristics with a biophysical model. Biophys J 1993; 64:803–812.
32. Bandettini PA, Wong EC, Jesmanowicz A, Hinks RS, Hyde JS. Simultaneous mapping of activation-induced $\Delta R2^*$ and $\Delta R2$ in the human brain using a combined gradient-echo and spin-echo EPI pulse sequence. In: Proceedings of the 12th annual meeting of the Society of Magnetic Resonance in Medicine. New York: Society of Magnetic Resonance in Medicine, 1993; 169.
33. Bandettini PA, Wong EC, Cox RW, Jesmanowicz A, Hinks RS, Hyde JS. Simultaneous assessment of blood oxygenation and flow contribution to activation-induced signal changes in the human brain. In: Proceedings of the 2nd annual meeting of the Society of Magnetic Resonance. San Francisco: Society of Magnetic Resonance, 1994; 439.
34. VanKylen J, Donahue K, Luh W-M, et al. Alternating TE interleaved gradient-echo/spin-echo EPI of graded ischemia in human skeletal muscle. In: Proceedings of the 5th annual meeting of the International Society for Magnetic Resonance in Medicine. Vancouver: International Society for Magnetic Resonance in Medicine, 1997; 24.
35. Patterson GC, Whelan RF. Reactive hyperemia in the human forearm. Clin Sci 1955; 14:197–211.
36. Johnson PC, Burton KS, Henrich H, Henrich U. Effect of occlusion duration on reactive hyperemia in sartorius muscle capillaries. Am J Physiol 1976; 230:715–719.
37. Gray SD, Renkin EM. Microvascular supply in relation to fiber metabolic type in mixed skeletal muscles of rabbits. Microvasc Res 1978; 16:406–425.
38. Weisskoff RM, Zuo CS, Boxerman JL, Rosen BR. Microscopic susceptibility variation and transverse relaxation: theory and experiment. Magn Reson Med 1994; 31:601–610.
39. Hoppel BE WR, Thulborn KR, Moore JB, Kwong KK, Rosen BR. Measurement of regional blood oxygenation and cerebral hemodynamics. Magn Reson Med 1993; 30:715–723.
40. Hyman C, Ballard K, Fielding P. Evidence for the shift of blood to the nutritive circulation during reactive hyperemia. Physiologist 1963; 6:206.
41. Shepherd JT. Reactive hyperemia in human extremities. Circ Res 1964; 1(suppl):76–79.
42. Boxerman J, Bandettini P, Kwong K, et al. The intravascular contribution to fMRI signal change: Monte Carlo modeling and diffusion-weighted studies in vivo. Magn Reson Med 1995; 34: 4–10.
43. Li D, Dhawale P, Rubin PJ, Haacke EM, Gropler RJ. Myocardial signal response to dipyridamole and dobutamine: demonstration of the BOLD effect using a double-echo gradient echo sequence. Magn Reson Med 1996; 36:16–20.
44. Fewings JD, Hyman C, Walsh JA, Whelan RF. The role of forearm skin and muscle vessels in reactive hyperaemia. Aust J Exp Biol Med Sci 1970; 48:179–186.
45. Hampson NB, Piantadosi CA. Near infrared monitoring of human skeletal muscle oxygenation during forearm ischemia. J Appl Physiol 1988; 64:2449–2457.
46. Biorck G, Sweden M. Hematin compounds in mammalian heart and skeletal muscle. Am Heart J 1956; 52:624–639.
47. Weisskoff RM, Kiihne S. MRI susceptometry: image-based measurement of absolute susceptibility of MR contrast agents and human blood. Magn Reson Med 1992; 24:375–383.